JAAS

Cite this: *J. Anal. At. Spectrom.*, 2012, **27**, 1391

www.rsc.org/jaas

PAPER

Improved *in situ* Hf isotope ratio analysis of zircon using newly designed X skimmer cone and jet sample cone in combination with the addition of nitrogen by laser ablation multiple collector ICP-MS

Zhaochu Hu,*[a] Yongsheng Liu,[a] Shan Gao,[a] Wengui Liu,[a] Wen Zhang,[a] Xirun Tong,[a] Lin Lin,[a] Keqing Zong,[a] Ming Li,[a] Haihong Chen,[a] Lian Zhou[a] and Lu Yang[b]

Received 5th March 2012, Accepted 2nd July 2012
DOI: 10.1039/c2ja30078h

The effect of three different cone combinations on the performance of laser ablation MC-ICP-MS (Neptune plus) for the *in situ* Hf isotope analysis of zircon were investigated. The signal sensitivities of Hf, Yb and Lu were improved by a factor of 1.4 and 2.5, respectively, with using the X skimmer cone + standard sampler cone and the X skimmer cone + Jet sample cone compared to the standard arrangement (H skimmer cone + standard sample cone). However, when using the high-sensitivity Jet sample cone, the instrumental mass fractionation for hafnium displayed a large non-linear component that could not be corrected using the normal mass fractionation laws. The magnitude of this non-linear mass fractionation was strongly related to the central gas flow rate. The *in situ* Hf isotope analysis of zircon standards 91500 and Mud Tank using the Jet cone displayed large deviations (410–470 ppm) at the optimum central gas flow rate for Hf, which seriously deteriorated the performance of the Jet cone. The addition of 4 ml min^{-1} nitrogen to the central gas flow in laser ablation MC-ICP-MS was found to not only increase the sensitivity of Hf by a factor of 2.1, but also suppress this non-linear mass fractionation. The determined Yb/Hf and Lu/Hf ratios at their corresponding optimum makeup gas flow rates for Hf intensity were found to be reduced by factors of 2 and 1.3 in the presence of nitrogen, respectively, which would benefit the accurate *in situ* determination of Hf isotopes in high-content Yb and Lu samples. Compared to the standard arrangement, the corresponding precision (2σ) of $^{176}Hf/^{177}Hf$ for single spot analysis of zircon standard 91500 was improved from 224 ppm to 50 ppm by using the newly designed X-skimmer cone and Jet sample cone in combination with the nitrogen addition technique. The determined $^{176}Hf/^{177}Hf$ ratios are in excellent agreement with published values in five reference zircon standards (91500, GJ-1, Mud Tank, Penglai and Plešovice). Our first Hf isotopic results from zircon standard M257 (0.281544 ± 0.000018; 2SD, $n = 151$) showed that it was fairly homogeneous in Hf isotopes. These results clearly demonstrate that the present analytical method has the potential to become an important tool for the pursuit of high-quality *in situ* Hf isotope data for zircons.

Introduction

Zircon ($ZrSiO_4$) is a common accessory mineral in a wide variety of rocks. It typically incorporates 0.5–2 wt% Hf into its crystal structure and controls the bulk rock Hf budget of most crustal rocks. Due to the extremely low Lu/Hf ratio (the $^{176}Lu/^{177}Hf$ ratio is typically <0.002) in zircon, the radiogenic ingrowth of ^{176}Hf from the beta decay of ^{176}Lu is negligible. Thus, the $^{176}Hf/^{177}Hf$ ratio found in zircon can be regarded as the initial value from when it crystallised. Zircon commonly preserves a very complex growth history. The high zircon Hf closure temperature (>1079 °C) indicates that Hf has remained isotopically closed during most later thermal events, even during high-grade metamorphism.[1,2] It has been well recognized that the zircon Lu–Hf isotopic system is a powerful tool for deciphering the evolution of the crust and mantle of the Earth.[3,4]

Generally, Hf isotope measurements are performed by MC-ICP-MS after dissolving the bulk sample and separating the pure Hf from other interfering and matrix elements.[5,6] However, these procedures are tedious and time-consuming. In the case of zircon analysis, any spatial information of Hf isotope in zircon is lost

[a]*State Key Laboratory of Geological Processes and Mineral Resources, China University of Geosciences, Wuhan, 430074, PR China. E-mail: zchu@vip.sina.com; Fax: +86 27 67885096; Tel: +86 27 61055600*
[b]*Measurement Science and Standards, National Research Council Canada, Ottawa, Ontario, K1A 0R6, Canada*

because the entire grain is digested. Geochemists are now increasingly interested in the *in situ* determination of Hf isotope ratios in zircon because the inherited cores and metamorphic overgrowths of zircon can be used to identify and distinguish various protoliths and geological processes from which the zircon was formed or later modified. Thirlwall and Walder[7] first demonstrated the potential of the laser ablation MC-ICP-MS (LA-MC-ICP-MS) technique for *in situ* zircon Hf isotope ratio determination. Recent improvements in instrumentation and methodology demonstrate that LA-MC-ICP-MS has become a powerful tool for *in situ* Hf isotope ratio measurements on single grains of zircon.[2,4,8–17] It is also worth noting that LA-MC-ICP-MS is currently the only method to determine *in situ* Hf isotopic compositions.

To improve the precision and accuracy of *in situ* Hf isotope analyses of zircon and to apply the technique to small or isotopically heterogeneous zircons, a higher analytical sensitivity is required. To obtain the desired precision and accuracy, a high energy density of laser ablation (10–25 J cm^{-2}) is usually adopted for the Hf isotope analysis of zircon.[2,11,13,15,16] However, such an approach increases the amount of consumed zircon and the chance of element fractionation during laser ablation, and is therefore not suitable for high spatial/depth resolution analysis. Thus, it would be ideal to increase the analytical sensitivity of the MC-ICP-MS instrument instead. In the quest to enhance the analytical capabilities, additional gases and solvents (*e.g.*, N_2, H_2, methane, methanol, and water) other than argon that bleed into one of the three gas flows of ICP have been studied in LA-ICP-MS.[13,18–25] Nitrogen is a popular gas used in LA-ICP-MS to improve sensitivity and stability, and to reduce oxide interferences. Durrant[18] first reported that the addition of approximately 1% v/v N_2 to the coolant flow or the addition of approximately 12% N_2 to the cell gas increased the Ce^+ and Th^+ signal sensitivities by a factor of 2–3 and reduced the CeO^+/Ce^+ and ThO^+/Th^+ ratios by a factor of 2–3 in LA-ICP-MS. Nesbitt *et al.*[19] also reported the enhanced sensitivity of heavy mass elements by roughly a factor of 10 (>100 amu) with the addition of small amounts of N_2 (0.4 ml min^{-1}) into the carrier gas in LA-ICP-MS, whereas the signal intensities of the low mass elements were suppressed by a factor of 5. Hu *et al.*[22] reported that the addition of 5–10 ml min^{-1} nitrogen to the central channel gas in LA-ICP-MS increased the sensitivity for most of the 65 investigated elements by a factor of 2 to 3 and decreased the oxide (ThO^+/Th^+) and hydride ratios (ArH^+/Ar^+) by a factor of 3 to 10. Compared to the spatial profiles of the ion distributions in the normal mode (without nitrogen), the addition of 5 ml min^{-1} nitrogen led to significantly wider axial profiles and more uniform distributions of ions with different physical and chemical properties.[22,23] Shaheen and Fryer[24] reported that the addition of N_2 to Ar carrier gas before the ablation cell in femtosecond laser ablation MC-ICP-MS improved the intensity of Tl and Pb by a factor of 3 to 4. This N_2 mixing technique has successfully been used to improve the precision and accuracy of the *in situ* Hf isotope microanalysis of zircon using LA-MC-ICP-MS[13] and occasionally used in elements analysis by LA-ICP-MS.[23]

It has been documented that the design and construction of the sample and skimmer cones makes a significant impact on the analytical sensitivity and instrumental mass fractionation behaviour.[26–39] For example, newly designed sample (Jet) and skimmer cones (X) have improved sensitivity for the Neptune (Thermo Electron Corp., Bremen, Germany) MC-ICP-MS, particularly for the light elements.[30] Numerous parameters such as the orifice size, the height, the material, the internal and external angles of the cone, and the distance between the sample and skimmer cones[26–39] all have significant impact on the performance of cones. However, the effect of the geometry and structure of the cones on analyte signal is usually element specific. In addition, the interface pressure can affect their performances.[30,31] In this study, we systematically investigated the effects of three different cone combinations, an H skimmer cone + standard sample cone, an X skimmer cone + standard sample cone, and an X skimmer cone + Jet sample cone, with or without the addition of nitrogen on the performance of LA-MC-ICP-MS (Neptune plus) for the *in situ* Hf isotope analysis of zircon.

Experimental

Instrumentation

Experiments were conducted using a Neptune Plus MC-ICP-MS (Thermo Fisher Scientific, Germany) in combination with a Geolas 2005 excimer ArF laser ablation system (Lambda Physik, Göttingen, Germany) at the state Key Laboratory of Geological Processes and Mineral Resources, China University of Geosciences in Wuhan, China. The Neptune Plus is a double focusing multi-collector ICP-MS that is equipped with seven ion counters, eight motorised Faraday cups and one fixed central Faraday cup that can be exchanged with an ion counter. The maximum distance between the outmost cup positions corresponds to a relative mass range of ~17%. Detailed descriptions for Neptune can be found in an early study by Weyer and Schwieters.[40] The Neptune Plus is a major update of the Neptune MC-ICP-MS platform. Among the new features are the use of a large dry interface pump (100 m^3 h^{-1} pumping speed), the newly designed X skimmer cone and Jet sample cone.[30] These cones are commercially available for use with the Neptune Plus MC-ICP-MS. However, the detailed information such as the geometry and structure of these cones is confidential. Three different combinations of cones were used in this study, including an H skimmer cone + standard sample cone, an X skimmer cone + standard sample cone and an X skimmer cone + Jet sample cone.

The Geolas 2005 laser ablation system consists of a COMPexPro 102 ArF excimer laser (wavelength of 193 nm, maximum energy of 200 mJ, and maximum pulse repetition rate of 20 Hz) and a MicroLas optical system. Its optical configuration allows for the selection of a constant fluence that is independent of the crater diameters. The energy density used in this study was 5.3 J cm^{-2}. The ultra-violet wavelength of 193 nm laser has been shown to yield superior control during ablation and smaller particle sizes, thereby leading to less elemental fractionation in LA-ICP-MS in comparison to the traditional 266 nm and 213 nm wavelength laser.[41,42] Helium was used as the carrier gas within the ablation cell and was merged with argon (makeup gas) after the ablation cell. As demonstrated by previous studies,[41,43,44] a 2 to 5-fold signal enhancement was consistently achieved in helium than in argon gas for the 193 nm laser. All data were acquired on

zircon in single spot ablation mode. Each measurement consisted of 20 s of acquisition of the background signal followed by 50 s of ablation signal acquisition.

Details of the instrumental operating conditions and measurement parameters are summarized in Table 1.

Addition of nitrogen

A simple Y junction was used downstream from the sample cell to add small amounts of nitrogen to the argon makeup gas flow.[22] The additional gas flow was controlled by a mass flow controller (Aalborg DFC 26 mass flow controller) with a range of up to 50 ml min^{-1}. Prior to MC-ICP-MS acquisition, the additional gas flow was increased to the desired values (2 ml min^{-1} or 4 ml min^{-1}) over approximately 10 min.

Correction for interferences by Lu and Yb

The major limitation to accurate *in situ* zircon Hf isotope determination by LA-MC-ICP-MS is the very large isobaric interference from ^{176}Yb and, to a much lesser extent ^{176}Lu on ^{176}Hf.[11] It has been shown that the mass fractionation of Yb (β_{Yb}) is not constant over time and that the β_{Yb} obtained from the introduction of solutions is unsuitable for *in situ* zircon measurements.[2,11,13,15] The under- or over-estimation of the β_{Yb} value would undoubtedly affect the accurate correction of ^{176}Yb and thus the determined $^{176}Hf/^{177}Hf$ ratio.[11] As proposed by many researchers,[2,11,15] the directly obtained β_{Yb} value from the zircon sample itself in real-time was applied in this study. The $^{179}Hf/^{177}Hf$ and $^{173}Yb/^{171}Yb$ ratios were used to calculate the mass bias of Hf (β_{Hf}) and Yb (β_{Yb}), which were normalised to $^{179}Hf/^{177}Hf = 0.7325$ and $^{173}Yb/^{171}Yb = 1.13017$ (ref. 45) using an exponential correction for mass bias. Interference of ^{176}Yb on ^{176}Hf was corrected by measuring the interference-free ^{173}Yb isotope and using $^{176}Yb/^{173}Yb = 0.79381$ (ref. 45) to calculate $^{176}Yb/^{177}Hf$. Similarly, the relatively minor interference of ^{176}Lu on ^{176}Hf was corrected by measuring the intensity of the interference-free ^{175}Lu isotope and using the recommended $^{176}Lu/^{175}Lu = 0.02656$ (ref. 5) to calculate $^{176}Lu/^{177}Hf$. The mass bias of Yb (β_{Yb}) was used to calculate the mass fractionation of Lu because of their similar physicochemical properties. Off-line selection and integration of analyte signals, and mass bias calibrations were performed using ICPMSDataCal.[46]

Results and discussion

Effect on signal intensity

Fig. 1 illustrates the integrated average signal intensity of ^{180}Hf on zircon standard 91500 at a spot size of 44 μm as a function of makeup gas flow rate for the three different sample and skimmer cone combinations in both the normal and the nitrogen (2 to 4 ml min^{-1}) modes. Irrespective of the three different sample and skimmer cone combinations used, the optimum makeup gas flow rates with respect to the maximum signal intensity were all found to be negatively correlated with the N_2 gas flow rate. The addition of nitrogen leads to a significantly wider axial ion distribution,[22] which might have accounted for this phenomenon. The optimum makeup gas flow rates of ^{180}Hf were shifted to a lower makeup gas flow rate by approximately 0.15 l min^{-1} for each 2 ml min^{-1} increase in the nitrogen gas flow rate in the H skimmer cone and standard sample cone combination mode (Fig. 1a). In contrast, the optimum makeup gas flow rates shifted by only approximately 0.10 l min^{-1} in the X skimmer cone and standard sample cone or the X skimmer cone and Jet sample cone combination modes for each 2 ml min^{-1} nitrogen gas flow rate increase (Fig. 1b and c). It should be noted that the use of the Jet sample cone resulted in the optimum makeup gas flow rate shifting to a lower makeup gas flow rate by approximately 0.15 l min^{-1} compared to the standard sample cone mode (Fig. 1). This

Table 1 Summary of the operating conditions that were used for LA-MC-ICP-MS measurements

Neptune plus MC-ICP-MS	
RF power	1270 W
Plasma gas flow rate	16.0l min^{-1}
Auxiliary gas flow rate	0.95l min^{-1}
Interface cones	a. H skimmer cone + standard sample cone b. X skimmer cone + standard sample cone c. X skimmer cone + Jet sample cone
Instrument resolution	~400 (low)
Detection system	Nine faraday collectors
Integration time	1 s, total time 70 s
Mass analyzer pressure	5–9 × 10^{-9} mbar
Masses analyzed in Faradays	171(Yb), 173(Yb), 174(Hf + Yb), 175(Lu), 176(Hf + Yb + Lu), 177(Hf), 179(Hf), 180(Hf + W), 182(W)
GeoLas 2005 laser ablation system	
Wavelength	193 nm, excimer laser
Pulse length	15 ns
Energy density	5.3 J cm^{-2}
Spot sizes	44 μm
Laser frequency	8 Hz
Ablation cell gas	Helium (0.85l min^{-1})
Makeup gas	Argon (0.30–1.3l min^{-1})

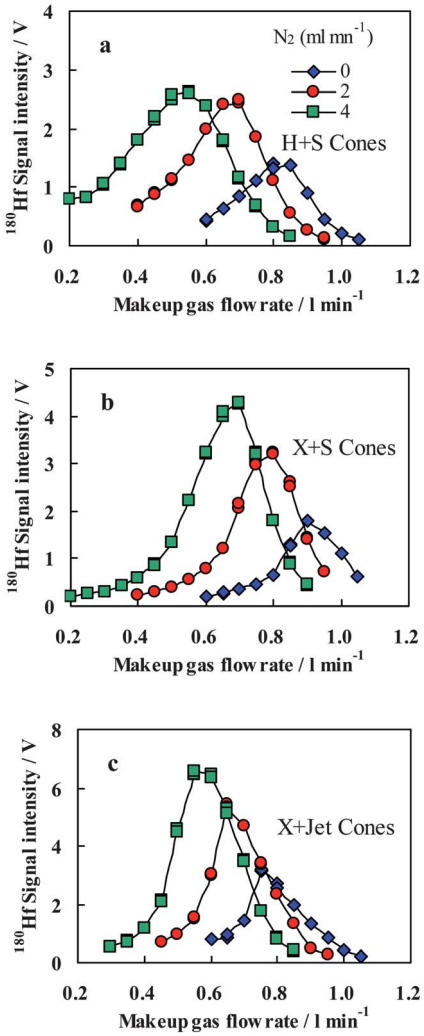

Fig. 1 The integrated average signal intensity of ^{180}Hf from zircon standard 91500 at a spot size of 44 μm as a function of makeup gas flow rate for the three different sample and skimmer cone combinations in both the normal and the nitrogen (N_2 = 2 and 4 ml min^{-1}) modes. (a) H skimmer cone + standard sample cone (H + S cones); (b) X skimmer cone + standard sample cone (X + S cones); (c) X skimmer cone + Jet sample cone (X + Jet cones).

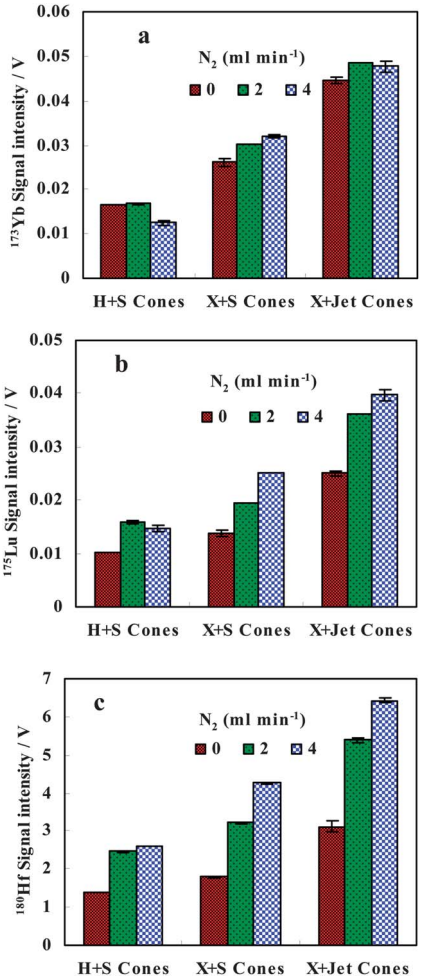

Fig. 2 Signal intensities of ^{173}Yb (a), ^{175}Lu (b) and ^{180}Hf (c) from zircon standard 91500 for the three different sample and skimmer cone combinations obtained both in the normal (N_2 = 0 ml min^{-1}) and nitrogen modes (N_2 = 2 and 4 ml min^{-1}) and their corresponding optimum makeup gas flow rates.

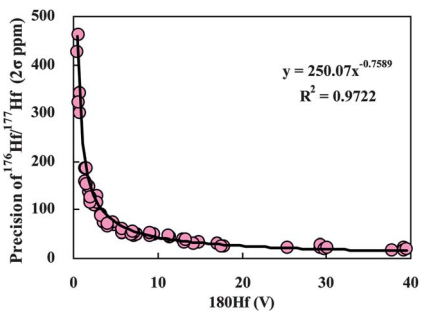

Fig. 3 The relationship between the ^{180}Hf signal intensity (the average signal of single spot analysis) and the precision of ^{176}Hf/^{177}Hf (2σ) for the *in situ* Hf isotope analyses of zircon standards 91500, GJ-1 and Mud Tank at different laser ablation spot sizes (16–90 μm).

is attributed to the increased height of the Jet sample cone in comparison with the standard sample cone, which results in the Jet sample cone tipping closer to the torch.

Fig. 2 shows the maximum signal intensities of ^{173}Yb, ^{175}Lu and ^{180}Hf (measured at their corresponding optimum makeup gas flow rates) from zircon standard 91500 for both the normal and the nitrogen modes using the three different sample and skimmer cone combinations. An improvement in analytical sensitivity was observed for all of the measured elements when using the X skimmer cone and standard sample cone or the X skimmer cone and Jet sample cone compared to the H skimmer cone and standard sample cone. The signal enhancement of these elements was 1.4 and 2.5 times for the X skimmer cone in combination with the standard sample cone and X skimmer cone in combination with the Jet sample cone in normal mode, respectively. The similar signal enhancement effects of these elements suggested that the increased signal intensities were mainly due to the increased ion extraction efficiency in the ICP by the modified design of the cones. Additionally, as shown in Fig. 2, the observed relative signal intensity after the addition

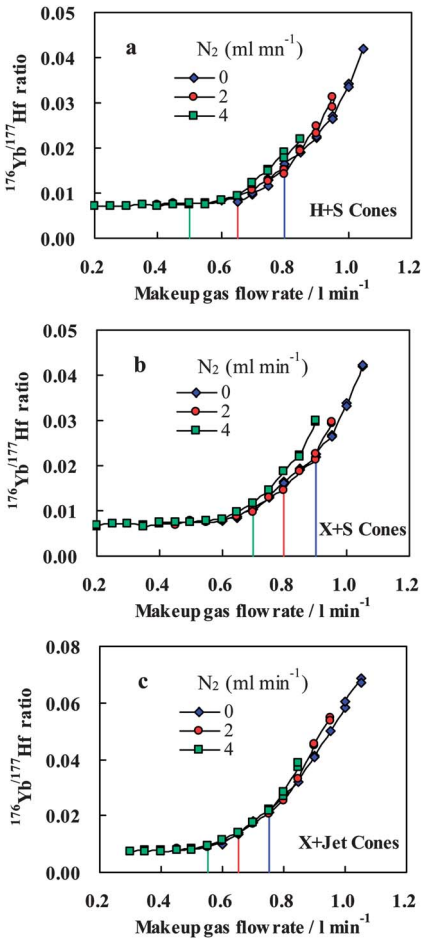

Fig. 4 Effect of makeup gas flow rate on the $^{176}Yb/^{177}Hf$ ratio for the three different sample and skimmer cone combination modes (a) H skimmer cone + standard sample cone; (b) X skimmer cone + standard sample cone; (c) X skimmer cone + Jet sample cone, both in the normal and the nitrogen ($N_2 = 2$ and 4 ml min^{-1}) in zircon standard 91500. The vertical lines show the optimum makeup gas flow rates for the normal and the nitrogen (2 and 4 ml min^{-1}) modes that yielded the maximum signal intensity for Hf^+.

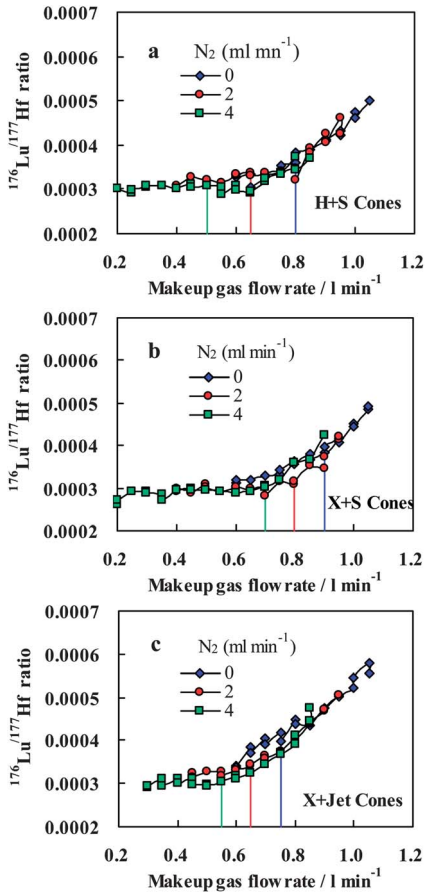

Fig. 5 Effect of makeup gas flow rate on the $^{176}Lu/^{177}Hf$ ratio for the three different sample and skimmer cone combination modes (a) H skimmer cone + standard sample cone; (b) X skimmer cone + standard sample cone; (c) X skimmer cone + Jet sample cone, both in the normal and the nitrogen ($N_2 = 2$ and 4 ml min^{-1}) in zircon standard 91500. The vertical lines show the optimum makeup gas flow rates for the normal and the nitrogen (2 and 4 ml min^{-1}) modes that yielded the maximum signal intensity for Hf^+.

of nitrogen was element-specific. For Yb, the addition of 2 and 4 ml min^{-1} nitrogen had a negligible effect on its signal intensity. In contrast, the maximum signal enhancement with the addition of nitrogen was 1.6 and 2.1 times for Lu and Hf, respectively, using these different skimmer and sample cone combinations. It has been reported previously that there is a roughly increasing trend of the signal enhancement factor with increasing ionisation potential by the addition of nitrogen in LA-ICP-MS.[22] In contrast, the signal enhancement factor obtained for Yb (6.25 eV) was less than that of Lu (5.42 eV) in this study. We believe that the evaporation enthalpy of the element may be another important parameter that must be considered. The evaporation enthalpies of these three elements are, in increasing order, Yb (129 kJ mol^{-1}), Lu (356 kJ mol^{-1}) and Hf (575 kJ mol^{-1}), which are positively related to their enhancement factors. It was reported in a previous study that N_2 has a thermal conductivity, which is higher than that of argon by a factor of 32 at 7000 K.[18] Therefore, it is possible

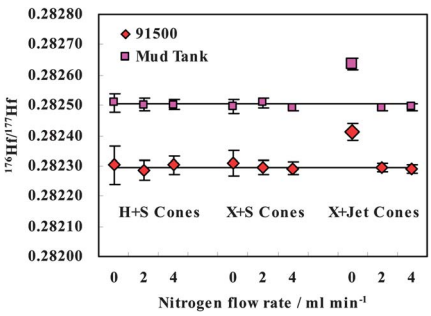

Fig. 6 The determined $^{176}Hf/^{177}Hf$ ratios in zircon standards 91500 and Mud Tank (measured at their corresponding optimum makeup gas flow rates for Hf) in both the normal and the nitrogen modes ($N_2 = 2$ to 4 ml min^{-1}) in three different sample and skimmer cone combinations. The horizontal lines delineate the reference values, which are taken from ref. 12.

that the increased sensitivity enhancements is due to the increased thermal conductivity, which would improve their evaporation in the ICP, especially for elements with high evaporation enthalpies.

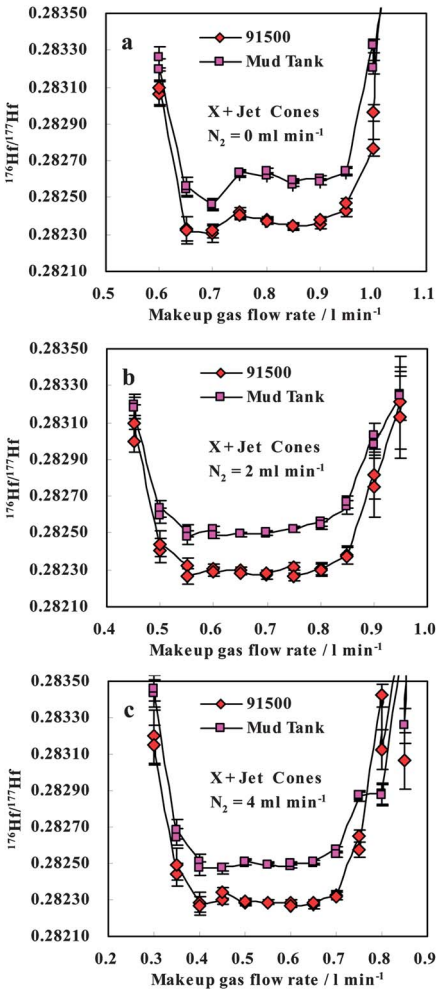

Fig. 7 Effect of makeup gas flow rate on the determined $^{176}Hf/^{177}Hf$ ratios in zircon standards 91500 and Mud Tank for the X skimmer cone in combination with Jet sample cone in the normal (a) and nitrogen (b and c) modes.

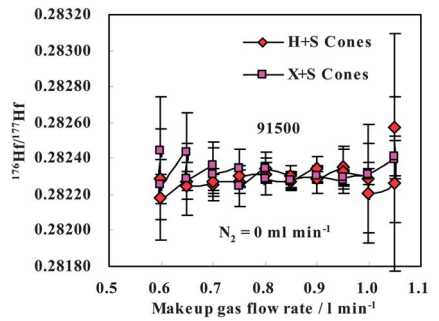

Fig. 8 Effect of makeup gas flow rate on the determined $^{176}Hf/^{177}Hf$ ratios on zircon standard 91500 and Mud Tank for the H skimmer cone or X skimmer cone in combination with the standard sample cone in the normal mode.

Intensity *vs.* precision

It is well known that the analytical precision is strongly dependent on the signal intensity. Woodhead *et al.*[11] have discussed in detail the theoretical limits of analytical precision of $^{176}Hf/^{177}Hf$ isotope, arising from amplifier noise, ion counting errors, and propagating errors from measurements of all appropriate isotopes (^{179}Hf, ^{177}Hf, ^{176}Hf, ^{176}Yb, ^{176}Lu, ^{175}Lu, ^{173}Yb, ^{171}Yb). Fig. 3 shows the relationship between the ^{180}Hf signal intensity (the average signal of single spot analysis) and the precision of $^{176}Hf/^{177}Hf$ (2σ) for *in situ* Hf isotope analyses of zircon standards 91500, GJ-1 and Mud Tank at different laser ablation spot sizes (16–90 μm) in this study. Clearly, the increase of the ^{180}Hf signal intensity from 0.5 V to 4 V led to a rapid improvement in the $^{176}Hf/^{177}Hf$ precision (2σ), followed by a more gradual improvement. Achieving ^{180}Hf signal intensity higher than 4 V is thus recommended for routine sampling of Hf isotope analysis. The correlation between the precision of $^{176}Hf/^{177}Hf$ (2σ) and the signal intensity of ^{180}Hf fit well into an exponential function (Fig. 3). Under the chosen instrument conditions, the best within-run precision (2σ) of $^{176}Hf/^{177}Hf$ was approximately 20 ppm (Fig. 3). These data strongly suggest that efforts should be made to improve the signal intensities for laser ablation analyses.

The efficient ways of achieving this improvement are to increase the spot size or the laser ablation energy density. However, these approaches are at the expense of the spatial and depth resolution and are ineffective in *in situ* zircon analysis due to its limited size. To overcome these limitations, it is necessary to increase the analytical sensitivity of the MC-ICP-MS instrument itself. As illustrated in Fig. 2, the use of the newly designed X skimmer cone and Jet sample cone in combination with the addition of nitrogen led to a signal enhancement factor of 2.4, 4.0 and 5.3 for Yb, Lu and Hf, compared to the use of the H skimmer cone and standard sample cone, respectively. The corresponding precision (2σ) of $^{176}Hf/^{177}Hf$ for single spot analyses was improved from 224 ppm to 50 ppm for 91500 under our given instrument conditions. Clearly, this sensitivity enhancement is important for isotopic analyses using LA-MC-ICP-MS in which an improved precision or an increased spatial resolution is of importance.

Effect on Yb/Hf and Lu/Hf ratios

Interferences are of particular concern in laser ablation MC-ICP-MS, as sample material cannot be chemically treated prior to analysis to remove specific interfering elements. A major impediment to the *in situ* accurate determination of Hf isotope in zircon are the interferences from ^{176}Yb and ^{176}Lu on ^{176}Hf.[2,11,13,15] Fig. 4 and 5 show the $^{176}Yb/^{177}Hf$ and $^{176}Lu/^{177}Hf$ ratios, respectively, from zircon standard 91500 at a spot size of 44 μm as a function of makeup gas flow rate for the three different sample and skimmer cone combinations in both the normal and the nitrogen (2 and 4 ml min^{-1}) modes. The $^{176}Yb/^{177}Hf$ and $^{176}Lu/^{177}Hf$ ratios were found to be highly dependent on the makeup gas flow rate. The $^{176}Yb/^{177}Hf$ and $^{176}Lu/^{177}Hf$ ratios normally increased with increasing makeup gas flow rate, and this was particularly true for the $^{176}Yb/^{177}Hf$ ratio. Therefore, it can be assumed that selective vaporization occurred. The evaporation enthalpy of Hf (575 kJ mol^{-1}) is much higher than that of Yb (129 kJ mol^{-1}) and Lu (356 kJ mol^{-1}), which makes it more sensitive to changes in gas temperature. The increased makeup gas flow rate has a cooling effect on the central channel of the plasma, which subsequently caused the increased $^{176}Yb/^{177}Hf$ and $^{176}Lu/^{177}Hf$ ratios. This effect is especially

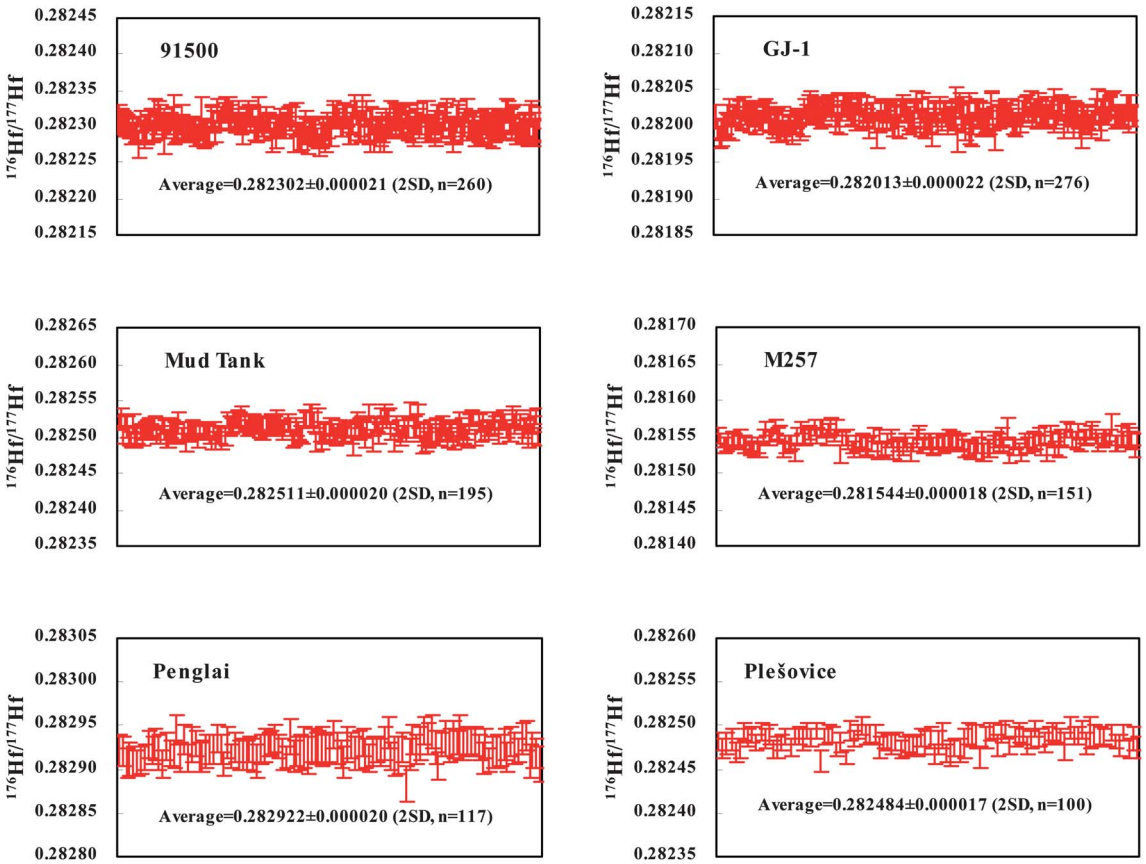

Fig. 9 A compilation of $^{176}Hf/^{177}Hf$ ratios that were obtained for six zircon reference materials during the course of this study (roughly a four month period). Error bars represent the within-run precision (2σ). Within each plot, the data are presented in chronological order.

significant for the X skimmer cone and Jet sample cone combination, which may be attributed to the plasma cooling effect that was caused by the increased extraction analyte amount because of its larger cone opening. Under optimum makeup gas flow rates, the $^{176}Yb/^{177}Hf$ ratio decreased from 0.0218 in the normal mode to approximately 0.00927 in the nitrogen mode (4 ml min^{-1}) (Fig. 4), and the $^{176}Lu/^{177}Hf$ ratio decreased from 0.000409 to 0.000304 (Fig. 5) for the X skimmer cone and Jet sample cone combination. As mentioned above, the lower $^{176}Yb/^{177}Hf$ and $^{176}Lu/^{177}Hf$ ratios in the presence of nitrogen may be attributed to a better energy transfer reaction, which would aid the accurate *in situ* determination of Hf isotopes in high-content Yb and Lu samples.

Non-linear mass dependent fractionation of Hf isotopes

It has been reported that Nd isotope ratios measured using the X cone on Neptune[29] or a high sensitivity skimmer cone on Nu Plasma[28] MC-ICP-MS instruments displayed large deviations (up to ~750 ppm) from the reference values. This deviation was not a linear function of mass, and therefore could not be corrected using the standard mass fractionation laws. Fig. 6 shows the determined $^{176}Hf/^{177}Hf$ ratios (measured at their corresponding optimum makeup gas flow rates for Hf intensity) on zircon standard 91500 and Mud Tank for both the normal and the nitrogen modes (2 and 4 ml min^{-1}) in three different sample and skimmer cone combinations. In the case of the Hf isotopes, the high-sensitivity Jet sample cone without nitrogen addition was found to contribute to a non-linear mass dependent fractionation that could not be corrected using the standard exponential laws. The measured $^{176}Hf/^{177}Hf$ ratios using the high-sensitivity Jet sample cone were found to deviate from the reference values by approximately 410 ppm and 470 ppm for zircon standards 91500 and Mud Tank, respectively (Fig. 6). This deviation could not be attributed to the incorrect interferences calibration of ^{176}Yb and ^{176}Lu on ^{176}Hf, because the $^{176}Yb/^{177}Hf$ (0.00188) and $^{176}Lu/^{177}Hf$ (0.0000537) ratios in zircon Mud Tank were extremely low. Furthermore, the observed $^{176}Hf/^{177}Hf$ deviation of 91500 should have been higher than that of Mud Tank because its $^{176}Yb/^{177}Hf$ (0.00927) and $^{176}Lu/^{177}Hf$ (0.000304) ratios were higher than those of Mud Tank by a factor of 5.0 and 5.6, respectively. Fig. 7 shows the effect of makeup gas flow rate on the determined $^{176}Hf/^{177}Hf$ ratios on zircon standard 91500 and Mud Tank for both the normal and the nitrogen modes (2 and 4 ml min^{-1}) in X skimmer cone and Jet sample cone combinations. It is evident that the measured $^{176}Hf/^{177}Hf$ ratios significantly increased at both lower and higher makeup gas flow rates, which was irrespective of the nitrogen addition. This type of phenomenon was unique in the case of the high-sensitivity Jet sample cone, since it was not observed in any of the H skimmer cone and standard sample cone or the X skimmer cone and standard sample cone combinations (Fig. 8). The determined $^{176}Hf/^{177}Hf$ ratio exhibited a W-shaped change as a function of makeup gas flow rate in normal mode (Fig. 7a). The accurate

$^{176}Hf/^{177}Hf$ ratios cannot be obtained at their corresponding optimum makeup gas flow rates for Hf intensity (Fig. 7a). Thus this type of non-linear mass-dependent fractionation introduced by the use of the high-sensitivity Jet sample cone severely deteriorated the *in situ* Hf isotope determination in zircon. Fortunately, this non-linear mass-dependent fractionation can be overcome by the addition of nitrogen at a certain extent. As illustrated in Fig. 7, the measured $^{176}Hf/^{177}Hf$ ratios were accurate at the optimum makeup gas flow rates and stable over a relatively large range of makeup gas flow rates in the presence of 2 and 4 ml min^{-1} nitrogen.

To date, only a limited number of studies[28,29,32,39] have been devoted to investigate the non-linear mass-dependent fractionation occurring in MC-ICP-MS. As a result the mechanisms of the non-linear mass dependent fractionation are not fully understood. Existing studies[28,29,32,39] have attributed this phenomenon to the nuclear field shift effect, magnetic isotope effect, oxide level or high first ionization potential of the element of interest. However, there are discrepancies in the literature in explaining the connection between the non-linear mass bias effects and the cone designs. For example, larger non-linear mass bias in Nd isotopes was reported with use of X cone compared to the standard high performance H cone.[29] Conversely, the magnitude of non-linear mass bias observed for W isotopes in another recent study was about 50% smaller with the use of high sensitivity X cone compared to the H cone.[32]

Newman[29] suggested that non-linear mass dependent fractionation observed for Nd isotopes could be attributed to the increased level of oxide formation when high sensitivity X cone is used. It is well known that the addition of a small amount of nitrogen to the carrier gas flow in LA-ICP-MS can significantly reduce the oxide formation.[18,22] Thus it is possible that this reduced level of oxide formation by the addition of nitrogen may partially account for the reduced non-linear mass dependent fractionation of Hf isotopes in this study. Further work on the non-linear mass dependent fractionation in the laser ablation MC-ICP-MS is needed to identify the specific mechanisms.

Results for zircon standard reference materials

Zircon standards 91500, GJ-1, Mud Tank, M257, Penglai and Plešovice have been widely used for the microbeam analyses of U–Pb age and to a lesser extent Hf–O isotopes.[2,11–17,47–59] Fig. 9 shows a compilation of the $^{176}Hf/^{177}Hf$ ratios that were obtained for these six zircon reference materials over the course of this study (approximately four months). The obtained results of zircon 91500 (0.282302 ± 0.000021; 2SD, n = 260), GJ-1(0.282013 ± 0.000022; 2SD, n = 276), Mud Tank (0.282511 ± 0.000020; 2SD, n = 195), Penglai (0.282922 ± 0.000020; 2SD, n = 117) and Plešovice (0.282484 ± 0.000017; 2SD, n = 100) agree with the recommended values[2,12,15,57,58] within 2σ error. The good agreement between the determined $^{176}Hf/^{177}Hf$ and the recommended values for the zircon standards not only validates the analytical protocol but also suggests that these zircons are homogeneous at this spatial level (44 μm). Our first Hf isotopic results for zircon M257 were very consistent (Fig. 9). Therefore, the M257 zircon is also fairly homogeneous in Hf isotopes. Combining all of the determined values, an average $^{176}Hf/^{177}Hf$ value of 0.281544 ± 0.000018 (2SD, n = 151) was obtained for zircon M257.

Conclusions

The selection of different sample and skimmer cones was shown to make a significant contribution to the analytical sensitivity and the mass fractionation behaviours in laser ablation MC-ICP-MS. Compared to the standard arrangement, the use of the newly designed X skimmer cone and Jet sample cone in combination with the addition of nitrogen improved the signal intensity of Hf, Yb and Lu by a factor of 5.3, 4.0 and 2.4, respectively. This sensitivity enhancement is important for the *in situ* Hf isotopic analysis of zircon using Faraday detectors where large ion beams are necessary for precise and accurate isotopic analyses. However, in the case of Hf, the high-sensitivity Jet sample cone geometry exhibited non-linear mass-dependent fractionation that was strongly related to the central gas flow rate and could not be corrected using normal mass fractionation laws. Fortunately, this anomalous mass fractionation effect was suppressed by the addition of 2 and 4 ml min^{-1} nitrogen in the central channel gas. The determined results for five reference zircon standards (91500, GJ-1, Mud Tank, Penglai and Plešovice) agreed well with the literature values. Our initial results from zircon standard M257 (0.281544 ± 0.000018; 2SD, n = 151) indicate that this material is fairly homogeneous in Hf isotopes. These results demonstrate that the presented analytical technique is capable of obtaining more reliable *in situ* Hf isotope data from zircon.

Acknowledgements

We would like to thank two reviewers for their constructive comments and Harriet Brewerton for overseeing the editorial process. This research is supported by the National Nature Science Foundation of China (Grants 41073020, 41271500, 90914007, 41173016 and 41125013), the Fundamental Research Funds for National Universities, the Program for New Century Excellent Talents in University (NCET-10-0754), the Fok Ying Tong Education Foundation (121017), the State Administration of the Foreign Experts Affairs of China (B07039), and MOST Special Fund from the State Key Laboratories of Geological Processes and Mineral Resources. We thank Xianhua Li and Yusheng Wan for providing the standard zircons.

References

1 D. J. Cherniak, J. M. Hanchar and E. B. Watson, *Mineral. Petrol.*, 1997, **127**, 383–390.
2 F. Y. Wu, Y. H. Yang, L. W. Xie, J. H. Yang and P. Xu, *Chem. Geol.*, 2006, **234**, 105–126.
3 P. D. Kinny and R. Maas, *Lu–Hf and Sm–Nd Isotope Systems in Zircon*, in Zircon, reviews in mineralogy and geochemistry, ed. J. M. Hanchar and P. W. O. Hoskin, 2003, vol. 53, pp. 327–341.
4 C. J. Hawkesworth and A. I. S. Kemp, *Chem. Geol.*, 2006, **226**, 144–162.
5 J. Blichert-Toft, C. Chauvel and F. Albarede, *Contrib. Mineral. Petrol.*, 1997, **127**, 248–260.
6 M. Bizzarro, J. Baker and D. Ulfbeck, *Geostand. Newsl.*, 2003, **27**, 133–145.
7 M. F. Thirlwall and A. J. Walder, *Chem. Geol.*, 1995, **122**, 241–247.
8 W. L. Griffin, N. J. Pearson, E. A. Belousova, S. E. Jackson, S. Y. O'Reilly, E. van Achterberg and S. R. Shee, *Geochim. Cosmochim. Acta*, 2000, **64**, 133–147.

9 W. L. Griffin, X. Wang, S. E. Jackson, N. J. Pearson, S. Y. O'Reilly, X. Xu and X. Zhou, *Lithos*, 2002, **61**, 237–269.
10 N. Machado and A. Simonetti, U–Pb Dating and Hf Isotopic Composition of Zircons by Laser Ablation-MC-ICP-MS, in *Laser-Ablation-ICPMS in the Earth Sciences: Principles and Applications*, ed. P. Sylvester, Mineralogical Association of Canada, 2001, vol. 29, pp. 121–146.
11 J. Woodhead, J. Hergt, M. Shelley, S. Eggins and R. Kemp, *Chem. Geol.*, 2004, **209**, 121–135.
12 J. Woodhead and J. M. Hergt, *Geostand. Geoanal. Res.*, 2005, **29**, 183–195.
13 T. Iizuka and T. Hirata, *Chem. Geol.*, 2005, **220**, 121–137.
14 K. J. Hou, Y. H. Li, T. R. Zou, X. M. Qu, Y. R. Shi and G. Q. Xie, *Acta Petrol. Sin.*, 2007, **23**, 2595–2604.
15 H. L. Yuan, S. Gao, M. N. Dai, C. L. Zong, D. Günther, G. H. Fontaine, X. M. Liu and C. R. Diwu, *Chem. Geol.*, 2008, **247**, 100–118.
16 L. W. Xie, Y. B. Zhang, H. H. Zhang, J. F. Sun and F. Y. Wu, *Chin. Sci. Bull.*, 2008, **53**, 1565–1573.
17 X. P. Xia, M. Sun, H. Y. Geng, Y. L. Sun, Y. J. Wang and G. C. Zhao, *J. Anal. At. Spectrom.*, 2011, **26**, 1868–1871.
18 S. F. Durrant, *Fresenius' J. Anal. Chem.*, 1994, **349**, 768–771.
19 R. W. Nesbitt, T. Hirata, I. B. Bilter and J. A. Milton, *Geostand. Newsl.*, 1997, **20**, 231–243.
20 M. Guillong and C. A. Heinrich, *J. Anal. At. Spectrom.*, 2007, **22**, 1488–1494.
21 Z. C. Hu, PhD Dissertation, Northwest University, Xi'an, 2006.
22 Z. C. Hu, S. Gao, Y. S. Liu, S. H. Hu, H. H. Chen and H. L. Yuan, *J. Anal. At. Spectrom.*, 2008, **23**, 1093–1101.
23 Z. C. Hu, Y. S. Liu, M. Li, S. Gao and L. S. Zhao, *Geostand. Geoanal. Res.*, 2009, **33**, 319–335.
24 M. Shaheen and B. J. Fryer, *J. Anal. At. Spectrom.*, 2010, **25**, 1006–1013.
25 D. Fliegel, C. Frei, G. Fontaine, Z. C. Hu, S. Gao and D. Günther, *Analyst*, 2011, **136**, 4925–4934.
26 M. A. Vaughan and G. Horlick, *Spectrochim. Acta, Part B*, 1990, **45**, 1289–1299.
27 I. Brenner, J. Pacheco and M. Valiente, *J. Anal. At. Spectrom.*, 2009, **24**, 1558–1563.
28 K. Newman, P. A. Freedman, J. Williams, N. S. Belshawb and A. N. Halliday, *J. Anal. At. Spectrom.*, 2009, **24**, 742–751.
29 K. Newman, *J. Anal. At. Spectrom.*, 2012, **27**, 63–70.
30 C. Bouman, M. Deerberg and J. B. Schwieters, Thermo Fischer Scientific Application Note: 30187.
31 A. Makishima and E. Nakamura, *J. Anal. At. Spectrom.*, 2010, **25**, 1712–1716.
32 N. Shirai and N. Humayun, *J. Anal. At. Spectrom.*, 2011, **26**, 1414–1420.
33 H. Niu and R. S. Houk, *Spectrochim. Acta, Part B*, 1996, **51**, 779–815.
34 K. E. Jarvis, P. Mason, T. Platzner and J. G. Williams, *J. Anal. At. Spectrom.*, 1998, **13**, 689–696.
35 E. Colas, M. Valiente and I. Brenner, *J. Anal. At. Spectrom.*, 2004, **19**, 282–285.
36 H. P. Longerich, B. J. Fryer, D. F. Strong and C. J. Kantipuly, *Spectrochim. Acta, Part B*, 1987, **42**, 75–92.
37 N. Taylor and P. B. Farnsworth, *Spectrochim. Acta, Part B*, 2012, **69**, 2–8.
38 W. Ferguson and R. S. Houk, *Spectrochim. Acta, Part B*, 2006, **61**, 905–915.
39 L. Yang, Z. Mester, L. Zhou, S. Gao, R. E. Sturgeon and J. Meija, *Anal. Chem.*, 2011, **83**, 8999–9004.
40 S. Weyer and J. B. Schwieters, *Int. J. Mass Spectrom.*, 2003, **226**, 355–368.
41 D. Günther and C. A. Heinrich, *J. Anal. At. Spectrom.*, 1999, **14**, 1369–1374.
42 M. Guillong, I. Horn and D. Günther, *J. Anal. At. Spectrom.*, 2003, **18**, 1224–1230.
43 S. M. Eggins, L. P. J. Kinsley and J. M. G. Shelley, *Appl. Surf. Sci.*, 1998, **129**, 278–286.
44 Z. C. Hu, Y. S. Liu, S. Gao, S. H. Hu, R. Dietiker and D. Günther, *J. Anal. At. Spectrom.*, 2008, **23**, 1192–1203.
45 I. Segal, L. Halicz and I. T. Platzner, *J. Anal. At. Spectrom.*, 2003, **18**, 1217–1223.
46 Y. S. Liu, S. Gao, Z. C. Hu, C. G. Gao, K. Q. Zong and D. B. Wang, *J. Petrol.*, 2010, **51**, 537–571.
47 M. Wiedenbeck, P. Alle, F. Corfu, W. L. Griffin, M. Meier, F. Oberli, A. Vonquadt, J. C. Roddick and W. Speigel, *Geostand. Newsl.*, 1995, **19**, 1–23.
48 M. Wiedenbeck, J. M. Hanchar, W. H. Peck, P. Sylvester, J. Valley, M. Whitehouse, A. Kronz, Y. Morishita, L. Nasdala, J. Fiebig, I. Franchi, J. P. Girard, R. C. Greenwood, R. Hinton, N. Kita, P. R. D. Mason, M. Norman, M. Ogasawara, R. Piccoli, D. Rhede, H. Satoh, B. Schulz-Dobrick, O. Skar, M. J. Spicuzza, K. Terada, A. Tindle, S. Togashi, T. Vennemann, Q. Xie and Y. F. Zheng, *Geostand. Geoanal. Res.*, 2004, **28**, 9–39.
49 T. Hirata and R. W. Nesbitt, *Geochim. Cosmochim. Acta*, 1995, **59**, 2491–2500.
50 I. Horn, R. L. Rudnick and W. F. McDonough, *Chem. Geol.*, 2000, **164**, 281–301.
51 J. Košler, H. Fonneland, P. Sylvester, M. Tubrett and R. B. Pedersen, *Chem. Geol.*, 2002, **182**, 605–618.
52 H. L. Yuan, S. Gao, X. M. Liu, H. M. Li, D. Günther and F. Y. Wu, *Geostand. Geoanal. Res.*, 2004, **28**, 353–370.
53 S. E. Jackson, N. J. Pearson, W. L. Griffin and E. A. Belousova, *Chem. Geol.*, 2004, **211**, 47–69.
54 L. P. Black, S. L. Kamo, C. M. Allen, D. W. Davis, J. N. Aleinikoff, J. W. Valley, R. Mundil, I. H. Campbell, R. J. Korsch, I. S. Williams and C. Foudoulis, *Chem. Geol.*, 2004, **205**, 115–140.
55 J. Blichert-Toft, *Chem. Geol.*, 2008, **253**, 252–257.
56 L. Nasdala, W. Hofmeister, N. Norberg, J. M. Mattinson, F. Corfu, W. Dörr, S. L. Kamo, A. K. Kennedy, A. Kronz, P. W. Reiners, D. Frei, J. Kosler, Y. S. Wan, J. Götze, T. Häger, A. Kröner and J. W. Valley, *Geostand. Geoanal. Res.*, 2008, **32**, 247–265.
57 J. Sláma, J. Košler, D. J. Condon, J. L. Crowley, A. Gerdes, J. M. Hanchar, M. S. A. Horstwood, G. A. Morris, L. Nasdala, N. Norberg, U. Schaltegger, B. Schoene, M. N. Tubrett and M. J. Whitehouse, *Chem. Geol.*, 2008, **249**, 1–35.
58 X. H. Li, W. G. Long, Q. L. Li, Y. Liu, Y. F. Zheng, Y. H. Yang, K. R. Chamberlain, D. F. Wan, C. H. Guo, X. C. Wang and H. Tao, *Geostand. Geoanal. Res.*, 2010, **34**, 117–134.
59 Y. S. Liu, Z. C. Hu, K. Q. Zong, C. G. Gao, S. Gao, J. Xu and H. H. Chen, *Chin. Sci. Bull.*, 2010, **55**, 1535–1546.